Al-Azhar Bulletin of Science

Volume 34 | Issue 1 Article 10

2023
Section: Earth science

Petrology, Geochemistry And Mineralogy Of Alaskan Type Ultramafic-Mafic Intrusive Complexes: A Case Study Around Mikbi-Zayatit District, South Eastern Desert, Egypt

Omar A. Soliman
Raw material engineer, Emirates steel, UAE

Hatem M. El-Desoky
Geology Department, Faculty of Science, Al-Azhar University, Cairo P.O. Box 11884, Egypt., heldesoky@azhar.edu.eg

Mahmoud M. El-Rahmany
Geology Department, Faculty of Science, Al-Azhar University, Cairo P.O. Box 11884, Egypt

Hamada M. El-Awny
Geology Department, Faculty of Science, Al-Azhar University, Cairo P.O. Box 11884, Egypt

How to Cite This Article

Soliman, Omar A.; El-Desoky, Hatem M.; El-Rahmany, Mahmoud M.; and El-Awny, Hamada M. (2023) "Petrology, Geochemistry And Mineralogy Of Alaskan Type Ultramafic-Mafic Intrusive Complexes: A Case Study Around Mikbi-Zayatit District, South Eastern Desert, Egypt," *Al-Azhar Bulletin of Science*: Vol. 34: Iss. 1, Article 10.
DOI: https://doi.org/10.58675/2636-3305.1638

ORIGINAL ARTICLE

Petrology, Geochemistry and Mineralogy of Alaskan Type Ultramafic-Mafic Intrusive Complexes: A Case Study Around Mikbi-Zayatit District, South Eastern Desert, Egypt

Omar Abdelaziz Soliman [a], Hatem Mohamed El-Desoky [b,*], Mahmoud Mohamed El-Rahmany [b], Hamada Megaly El-Awny [b]

[a] Raw Material Engineer, Emirates Steel, United Arab Emirates
[b] Geology Department, Faculty of Science, Al-Azhar University, Cairo, Egypt

Abstract

The present work deals with the field geology, petrography, geochemistry and mineralogy of Wadi Zayatit and Wadi Mikbi ultramafic-mafic intrusive complex, South Eastern Desert, Egypt. Based on the current geological maps, field observations, structural relationships, and previous works; the rocks that exposed in the study regions are dunites, peridotites, and gabbro. These rocks characterized by coarse-grained, dark greyish to whitish grey color, massive with lustric features and slightly deformed with low to moderate relief. The commonest of the accessory constituents is an oxide ore mineral of some kinds, the most frequent one is chromite, ilmenite, titano-magnetite and magnesio-ferrite. The petrographic descriptions of each rock unit of the studied layered ultramafic-mafic intrusion are recognized; dunites, serpentinized peridotites, and olivine gabbro. Petrographically, opaque minerals are found as coarse-grained, euhedral crystals dispersed throughout the mineral constituents and represented by titani-ferous magnetite and chromite. Titano-magnetite has high FeO and low TiO_2. The Fe_2O_3 and TiO_2 show increase with decrease in silica content (SiO_2). These rock units have high contents of Ni (9767 ppm), Cr (7861 ppm), and Co (1525 ppm). The clino-pyroxene and bulk-rock chemistry indicates strongly crystallization from orogenic hydrous tholeiitic to calc-alkaline magmatic affinity. These inferences suggest that their primary magma was derived from partial melting of a mantle wedge source that has suffered metasomatism in a subduction zone setting. Ore microscopy, XRD technique, and EDX microchemical analysis of representative mineralized samples of ultramafic-mafic intrusive complex identified chromite, ilmenite, titano-magnetite, magnesio-ferrite and clinochlore.

Keywords: Alaskan type, Eastern desert, Geochemical characteristics, Ore mineralogy, Petrological study

1. Introduction

Wadi Zayatit and Wadi Mikbi is totally covered by Neoproterozoic basement rocks of the Southern Eastern Desert, and is bounded by Latitudes 24° 4' - 24° 10′N and Longitudes 35° 5' - 35° 15′E of roughly 200 000 000 Km^2 (Fig. 1). Mikbi-Zayatit intrusion is a part of the Neoproterozoic Nubian Shield located along the NE−SW trending major fracture zones prevailing southern Eastern Desert of Egypt Abdallah and colleagues [1]. Alaskan type ultramafic-mafic intrusive complexes, which are originated from the mantle magmas formed in a variety of tectonic contexts, can provide crucial insights into the tectonic movements. One of the most crucial aspects for understanding the genesis of tectonically complex terranes, understanding geodynamic environments, and understanding processes involving crust−mantle interaction is still the meticulous investigation of Neoproterozoic basement rocks Abd El-Wahed and

Received 25 December 2022; revised 12 January 2023; accepted 13 January 2023.
Available online 18 October 2023

* Corresponding author at: Geology Department, Faculty of Science, Al-Azhar University, Cairo P.O. Box 11884, Egypt.
E-mail address: heldesoky@azhar.edu.eg (H.M. El-Desoky).

https://doi.org/10.21608/2636-3305.1638

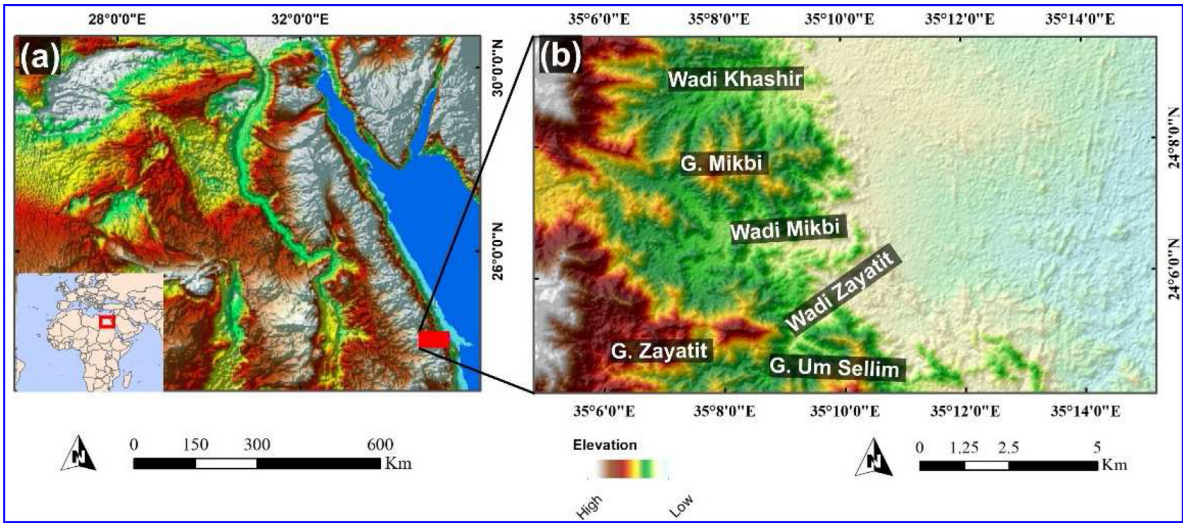

Fig. 1. (a) Location map of the study district, South Eastern Desert, Egypt. (b) ALOS PALSAR DEM of Wadi Zayatit and Wadi Mikbi district, South Eastern Desert, Egypt.

colleagues [2] especially in the South Eastern Desert. Tectonically, there have separated into North Eastern Desert (NED), which is primarily thought of as an extendable region, Central Eastern Desert (CED), South Eastern Desert (SED), where the regime of compression predominates and metamorphic domes are largely visible, is regarded as a wrench region Hamimi and colleagues [3]. Lithological assemblages of many types are produced by these diverse tectonic regimes in the SED, CED, and NED Hamimi and colleagues [3].

The area under research right now (Wadi Zayatit and Wadi Mikbi) belongs to the South Eastern Desert, Egypt. Numerous authors have already researched the South Eastern Desert Neoproterozoic basement rocks rocks Kotb and colleagues, Abdel-Karim and colleagues [4−9]. Magmas that form arcs and are grouped closely together with Alaskan type ultramafic-mafic intrusive complexes are a sign that the subducted slab is entering the mantle origin Helmy and colleagues, Pearce and Stern [7,10]. Alaskan type ultramafic-mafic intrusive complexes emerge as raised debris from the deep depths of island arcs along the main building Helmy and colleagues, Batanova and colleagues, Teng and colleagues [7,11,12].

2. Materials and methods

2.1. Field evidence and analytical techniques

Using a global positioning system (GPS) survey, more than 50 rock samples were collected from the lithological units of Alaskan type ultramafic-mafic intrusive complexes of the study district. Thin section prepared for the petrographic examination in the transmitted light. A total of 20 thin sections collected from the different rock units encountered in the studied area were analyzed petrographically under a polarized microscope to identify mineralogical composition and textural features. The chemical analyses as well as chemical determination of major oxides, trace elements, rare earth elements contents of the studied district were carried out at the laboratories of the Central Metallurgical Researching and Development Institute (CMRDI), Egypt. A laboratory jaw-crusher is used for crushing the samples then; an aliquot of the sample is ground to −200 mesh grain size to measure the major oxides concentrations by wet chemical analysis. The X-ray fluorescence technique (XRF) is used to determine the trace element concentrations (ppm) via PHILIPS X' Unique-II spectrometer with automatic sample changer PW 1510. This instrument is connected to a computer system using X-40 program for spectrometry.

The trace elements concentrations are calculated from the program's calibration curves, which are set up according to international reference materials (standards) as NIM-G, G-2, GSP-1, AGV-1, JB-1, and NIM-D. The detection limit for the elements measured by XRF technique is estimated at 2 ppm for Rb, Nb, Ga, Y, and Sr and at 8 ppm for Pb and Cu and 5 ppm for other measured trace elements. REEs are measured by using an Inductively Coupled Plasma Optical Emission Spectrometer (Prism ICP, Teledyne Technologies). A radio frequency generator is used to provide the power required for the generation and sustaining of the plasma discharge. The power used for optical emission spectrometer (OES) measurements is

1200 W. The sample is injected at the rate of 1.4 ml/min by using a peristaltic pump to concentric Nebulizer with Argon (Ar) carrier gas pressure 34 psi carrying the samples to an Axial cyclonic spray chamber with auxiliary Ar gas flow 0.1 L/min, which make spray and atomization for the sample before entering the torch. A coolant (Ar) gas with flow rate 18 L/min is used to prevent the torch over heat.

3. Field verification

A field observation of Alaskan type intrusions occupies the central northern part of Wadi Mikbi area and are coarse-grained, dark greyish to whitish grey color (Fig. 2). These rocks are massive with lustric features, and slightly deformed with low to moderate relief. The commonest of the accessory constituents is an oxide ore mineral of some kinds, the most frequent one is chromite and titanomagnetite.

Generally, the peridotites occur as ultramafic rocks and coarse-grained, dark to grey colored, composed more than 90% olivine and pyroxene. Peridotites are commercially significant rocks because they frequently contain magnetite and chromite minerals. Peridotites are thought to make up a sizable portion of the earth upper mantle. Peridotites found in sporadic slices inside metagabbro and granitic rocks and predominantly exposed at Wadi Zayatit district (in the middle southern region of the map). They occupy small areas and form conspicuous mountainous ridges with steep slopes. These rocks are generally massive but become sheared along shear zone. They found as shear pods or lens-like bodies within the enclosing rocks (Fig. 3c). These lenses range in length from 25 to 60 m and in width from 15 to 25 m. They are generally colored grey and dark green colors, in some spots; these rocks are quite sheared, massive; occasionally change into serpentinites and include small amounts of iron oxides (magnetite crystals) along the shear zones. Tectonized peridotites are altered to serpentinites and talc carbonate rock as the intensity of carbonatization increases near steeply dipping transpressive faults. The contacts between the peridotites and adjacent rocks (granitic rocks) are sharp and distinct (Fig. 3d).

The dunite rocks encountered in the central part of Wadi Mikbi area and are medium-to coarse-grained grey to whitish grey in color (Fig. 3a). They are composed essentially of olivine, pyroxene, plagioclase, and iron oxide (chromite). These rocks commonly highly jointed, fractured and

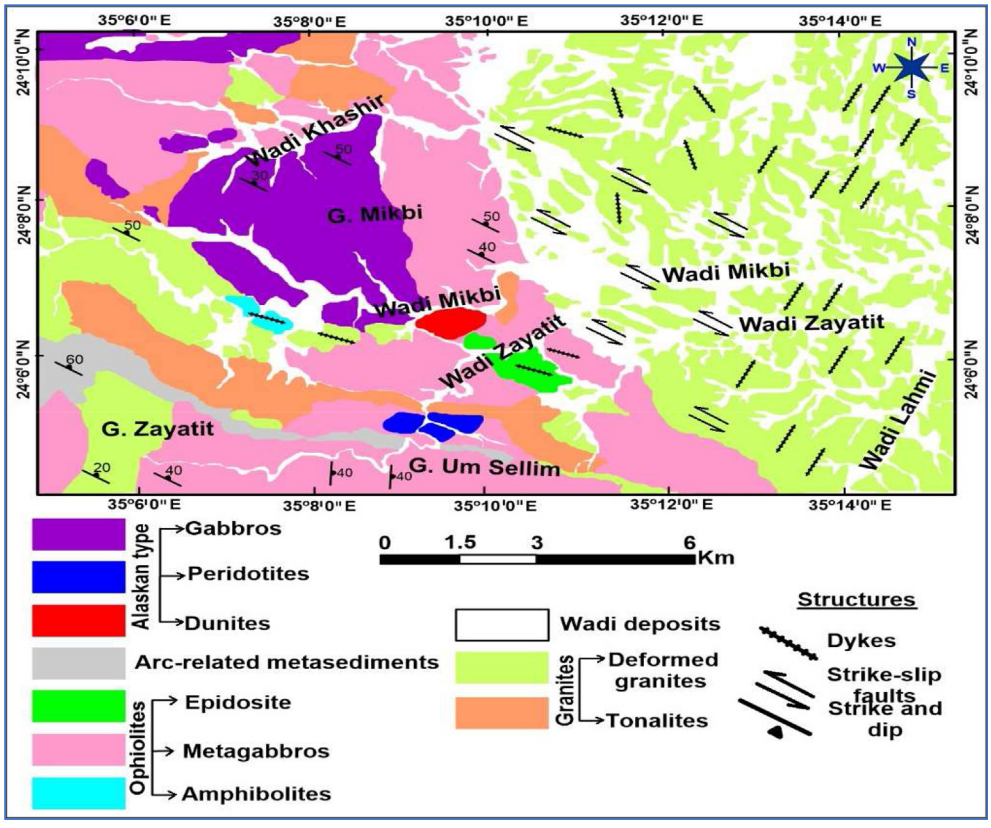

Fig. 2. Geological map of Wadi Zayatit and Wadi Mikbi district, South Eastern Desert, Egypt [1].

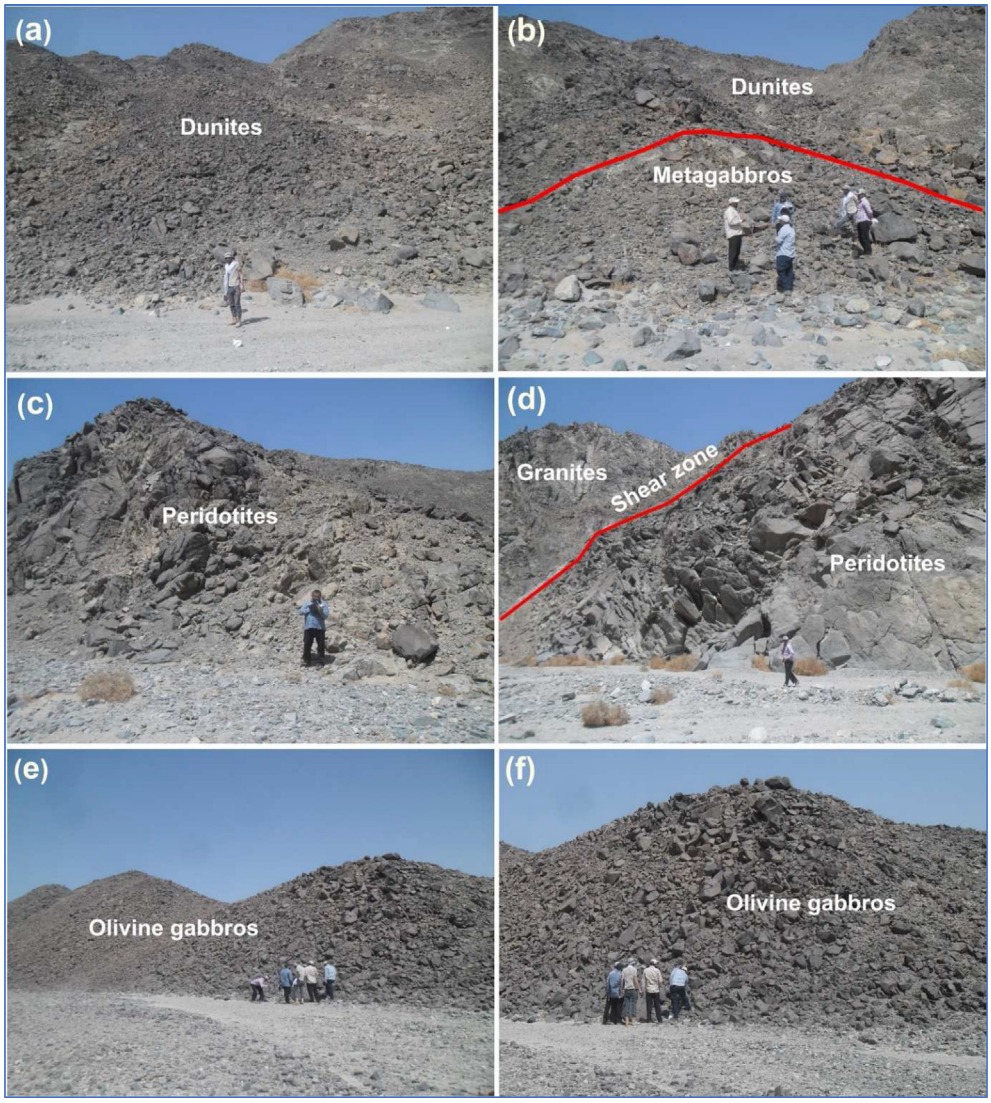

Fig. 3. Field observations of the Alaskan type ultramafic-mafic intrusive showing: (a) Medium to high relief of dunites. (b) Contact between ophiolitic metagabbros and dunites. (c) Massive and jointed peridotites. (d) Shear zone between peridotites and granites. (e) Spheroidal shape of weathered olivine gabbros. (f) Dark greenish color of fractured olivine gabbros.

characterized by medium to high relief. Dunites, also known as olivinite, are an intrusive mafic rock of ultramafic composition and coarse-grained texture. Over 90% of the mineral assemblage is olivine. These are in turn intruded by late intrusive dunite bodies and presence of small black chromite crystals. Field relationships shows these dunite bodies do not show intrusive contacts with the foliated ophiolitic metagabbro (Fig. 3b). Dunite rocks are considered the major constituents of the earth mantle above a depth of around 250 m. Most often, large layers of these 'cumulate' dunites are found in thick layers in layered intrusions, associated with cumulate layers of olivine, pyroxene, and chromite.

Olivine gabbro exposed at Wadi Mikbi region (in the Western and Southern West of the map). Olivine gabbro composed of a coarse grain of plagioclase, olivine, pyroxene, and iron oxides (titanomagnetite minerals). They have a fresh surface that is dark green to grey in color, homogeneous intrusion, massive with lustric characteristics and slightly deformed with moderate relief of west trend (Fig. 3e). It can occasionally take the shape of spheroidal weathered masses and is primly made up of coarse-grained of plagioclase, olivine, and pyroxene crystals. Olivine gabbro often have thicknesses between 10 and 20 m (Fig. 3f). These olivine gabbro are exhibits dark greenish weathered surface owing to its oxidation of titanomagnetite crystals.

The mafic intrusive gabbro represent some of the youngest undeformed plutonic rocks. It is represented by isometric-layered small masses intruded into the ophiolitic and granitic rocks (Fig. 3f).

4. Results and discussions

4.1. Petrographical studies

The rocks of Wadi Zayatit and Wadi Mikbi ultramafic-mafic intrusive complex are represented by dunites, peridotites, and gabbro. These rocks are of a layered igneous complex, markedly heterogeneous nature in its outcrop, and coarse-to very coarse-grained, and also exhibit pegmatoidal texture. The petrographic descriptions of each rock unit of the studied layered ultramafic-mafic intrusion are recognized below. Dunites are almost pure olivine rocks and consist of masses of strained and deformed closely knit olivine anhedral crystals. They are coarse-to very coarse-grained and composed principally of olivine with less amounts of plagioclase, pyroxene, and opaque. There are traces of chromium diopside and enstatite crystals around olivine crystals. These dunites suffered from two microfractures system that filled with opaque minerals and exhibit well-developed corona and symplectite textures. Corona texture occurs as well-developed olivine crystals surrounded by two zones of orthopyroxene and fibrous amphiboles reaction rims (Fig. 4a-c).

Olivine forms medium-to coarse-grained, high relief, equidimensional crystals, and partly altered to iddingsite (Fig. 4a). Olivine characteristically shows a network of cracks rather than cleavage, but sometimes the cleavage is quite well-developed. Sometimes olivine crystals show effects of post-consolidation reactions. Slow cooling in an almost dry environment may permit development of kelyphitic reaction rims

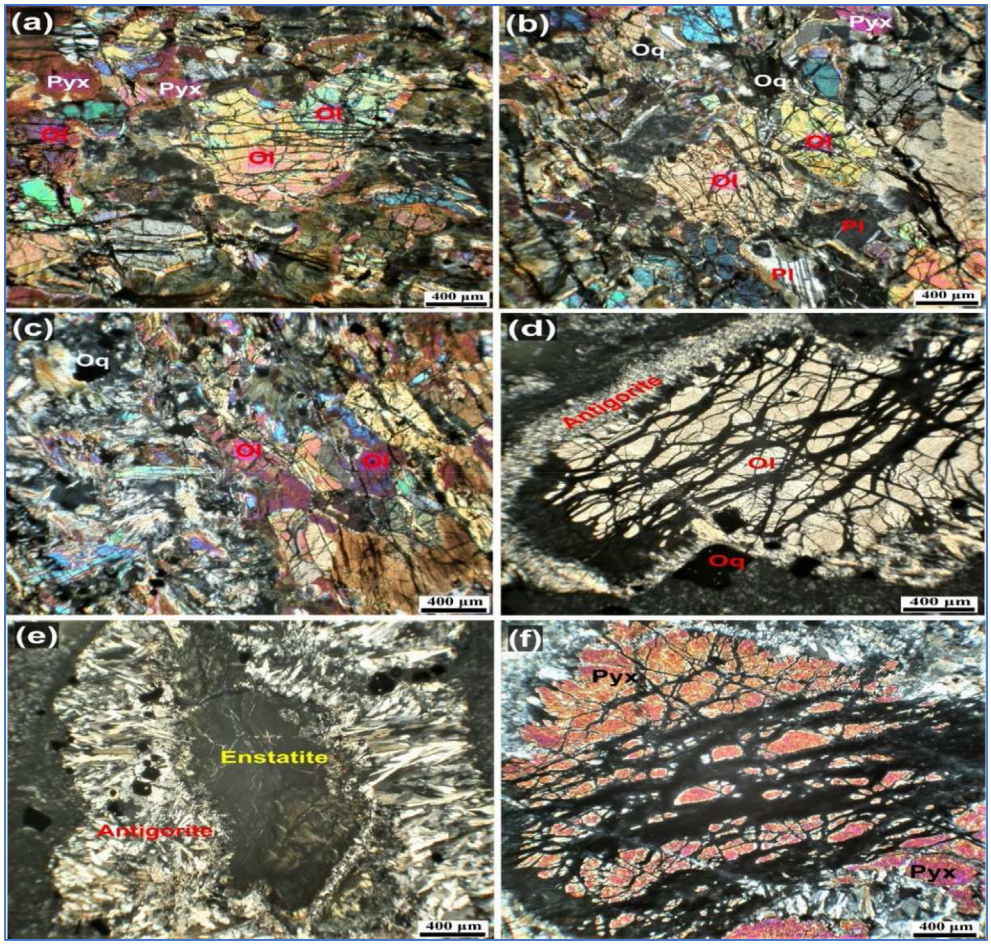

Fig. 4. Photomicrographs of the Alaskan type ultramafic-mafic intrusive complexes showing: (a) Olivine (Ol) oval-shaped crystals with pyroxene (Pyx) within dunites. (b) Plagioclase (Pl) lamellar twinning associated with olivine (Ol) crystals in dunites. (c) Opaque (Oq) crystals enclosed within olivine (Ol) of dunites. (d) 'Y' cracks crystal of olivine (Ol) encountered in peridotites. (e) Enstatite and antigorite crystals in peridotites. (f) Coarse-grained from pyroxene crystal (Pyx) in peridotites.

or corona (Fig. 4b) around the olivine consisting of orthopyroxene and fibrous amphiboles (whereas the peripheral zone of fibrous amphiboles and orthopyroxene would be in contact with olivine). Olivine is replaced by orthopyroxene-titanomagnetite symplectites. Orthopyroxene–titanomagnetite symplectite is developed at the immediate olivine phase boundary and is considered to be the oxidation product of olivine crystals (Fig. 4c). Small olivine anhedral crystals appear to be largely or entirely enclosed in the orthopyroxene (enstatite) and clinopyroxene (titanaugite) crystals (Fig. 4a & b).

Plagioclase typically is labradorite or bytownite (An_{40-80}), present as very coarse-grained, and subhedral tabular crystals (Fig. 4b). Sometimes, plagioclase is rather fresh with lamellar twinning but

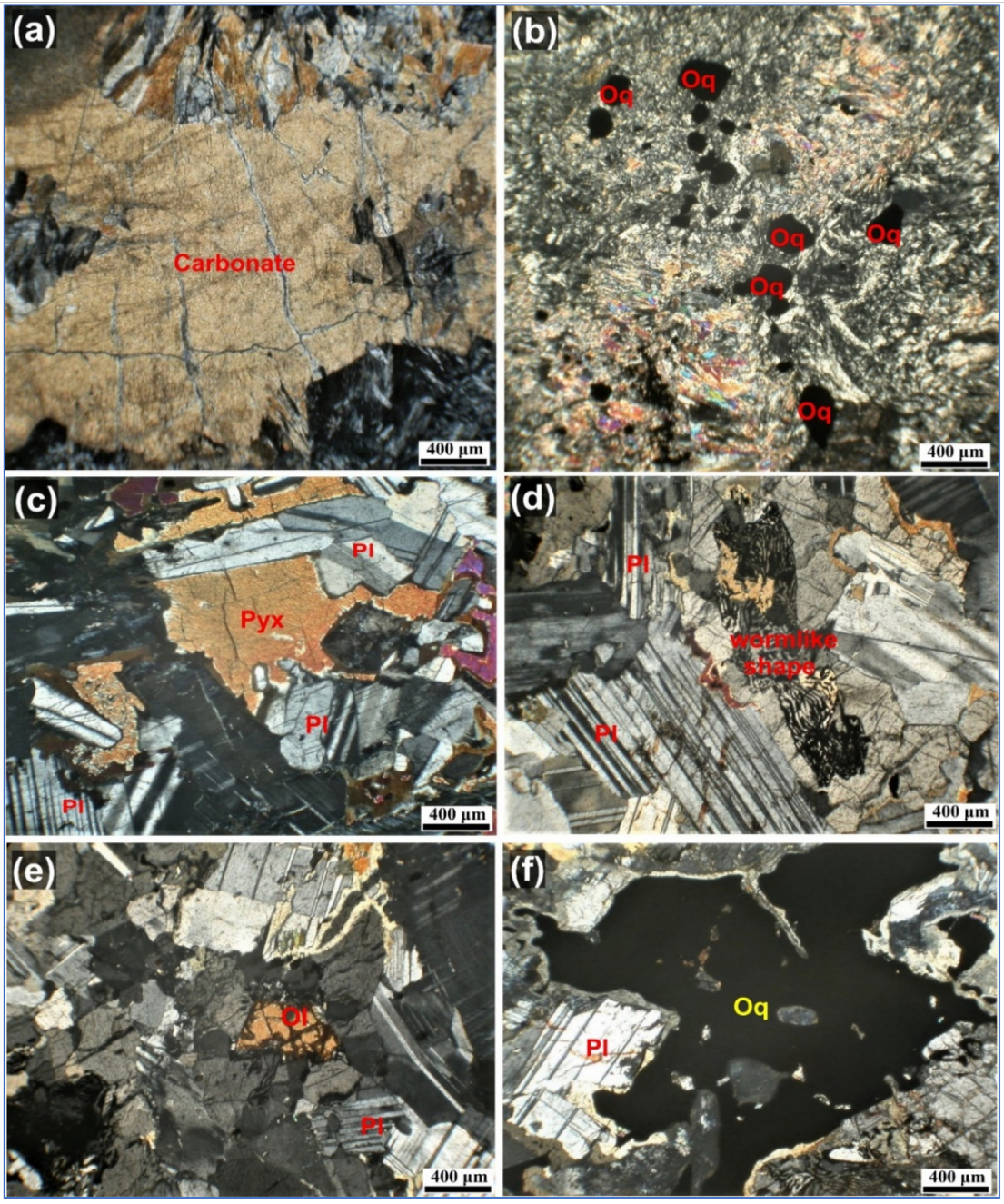

Fig. 5. Photomicrographs of the Alaskan type ultramafic-mafic intrusive complexes showing: (a) Aggregates of carbonate crystals in peridotites. (b) Opaque (Oq) crystals as inclusions in peridotites. (c) Subidiomorphic to xenomorphic of pyroxene (Pyx) crystals in olivine gabbros. (d) Plagioclase (Pl) lamellar twinning associated with worm-like opaque crystals in olivine gabbros. (e) Olivine (Ol) oval-shaped crystals with pyroxene (Pyx) in olivine gabbros. (f) Coarse-grained opaque (Oq) mineral crystals within the olivine gabbros.

occasionally is cloudy with alteration and with small inclusions of olivine crystals to give poikilitic texture (Fig. 4b). Clinopyroxene (titanaugite) and orthopyroxene (enstatite) occurs as coarse-grained, subhedral to anhedral crystals and it is frequently containing small inclusions of olivine crystals (Fig. 4c). Iddingsite occurs as partial or complete alteration pseudomorphs after olivine crystals. It is pale reddish yellow color and consists of iron oxides in various stages of oxidation and hydration processes in these dunites (Fig. 4c). Opaque minerals are represented by chrome-spinel and magnetite and it is filling the microfractures (Fig. 4c). Chromium magnetite is present as distinct grains in a corona. The two latter are more chrome rich spinels. Opaque commonly occur along the microcracks, or within the olivine and pyroxene grains. Sometimes, they are observed as platelets pseudomorphs after olivine crystals.

Serpentinized peridotites consists essentially of phenocrysts of olivine (forsterite) and two kinds of pyroxene (enstatite and diopside) in a groundmass, which commonly contains serpentine (antigorite), chrome spinel, magnetite, brucite, clinochlore, and immature carbonate minerals. Peridotites containing both orthopyroxene (enstatite) and clinopyroxene (diopside) are often called lherzolites. The large olivine phenocrysts are partly serpentinized and iddingsite. The groundmass is highly serpentinized. Around olivine and pyroxene phenocrysts in this peridotite there is a wide corona, which consists of either one or two zones. A radially oriented, fibrous, pale green antigorite zone is surrounded the olivine phenocrysts. The olivine phenocrysts have round outlines and surrounded by reaction rims of microcrystalline serpentine. Olivine found as coarse-to very coarse-grained, anhedral to subhedral phenocrysts (Fig. 4d). Olivine is present as forsterite in composition, and whereas the phenocrysts are commonly fresh, the groundmass olivine is usually more or less completely altered to serpentine (antigorite). Olivine partly alters to green irregular platy serpentine along the grain boundaries. The phenocrysts are slightly altered, especially along the cracks and borders (Fig. 4d). The

Table 1. Chemical analysis of major oxides, trace elements, and REE of the ultramafic-mafic intrusive complex.

Rock	Serpentinized peridotites						Dunites			Olivine gabbros			
S. No.	Z_{23}	Z_{24}	Z_{25}	Z_{26}	Z_{27}	Z_{30}	M_4	M_5	M_7	M_3	M_8	M_{13}	M_{14}
Major oxides (Wt. %)													
SiO_2	28.09	38.09	36.10	38.46	40.22	38.77	40.21	41.19	39.12	31.16	34.64	39.37	37.62
TiO_2	0.42	0.21	0.39	0.34	0.25	0.34	0.77	0.87	1.01	0.46	1.04	0.69	0.91
Al_2O_3	5.57	10.56	10.52	9.67	10.01	8.38	14.26	15.24	15.10	5.82	17.59	19.70	15.76
$Fe_2O_3^{tot}$	44.63	20.90	25.55	19.24	16.32	23.41	15.69	14.71	16.10	36.28	19.67	14.94	18.67
MnO	0.59	0.28	0.34	0.25	0.23	0.31	0.24	0.20	0.27	0.44	0.31	0.27	0.37
MgO	11.31	22.46	20.28	24.04	24.08	21.02	7.30	7.34	8.10	17.43	5.09	4.72	4.64
CaO	7.20	5.25	5.22	5.86	7.12	6.23	18.03	17.20	18.30	6.35	18.74	17.28	19.32
Na_2O	0.49	0.32	0.38	0.34	0.27	0.29	1.61	1.72	1.30	0.59	2.04	2.15	2.07
K_2O	0.08	0.03	0.05	0.02	0.02	0.02	0.09	0.08	0.07	0.06	0.12	0.10	0.09
P_2O_5	0.19	0.06	0.08	0.07	0.08	0.06	0.09	0.07	0.08	0.06	0.12	0.20	0.17
SO_3	0.18	0.16	0.13	0.19	0.14	0.15	0.12	0.13	0.15	0.07	0.15	0.18	0.09
Cl	0.00	0.11	0.00	0.09	0.00	0.10	0.00	0.00	0.00	0.00	0.15	0.17	0.00
L.O.I	1.23	1.56	0.90	1.33	1.24	0.88	1.30	1.21	1.00	1.20	0.00	0.00	0.00
Trace elements (ppm)													
Sc	2.03	10.14	8.88	9.86	14.79	8.12	44.04	44.09	41.12	8.19	18.34	22.95	28.33
Co	1525.77	534.81	456.16	456.16	298.86	589.86	291.00	290.10	288.21	833.67	377.51	338.19	306.73
Cr	7861.46	5343.60	4953.61	4590.98	4692.98	6431.48	711.57	710.50	715.20	1361.56	519.99	355.78	602.10
Cu	156.35	167.76	127.82	135.80	167.76	239.66	343.51	346.20	350.20	391.44	263.62	167.76	351.49
Ni	9767.99	3017.63	3064.78	2420.39	2019.61	3159.08	298.62	300.20	300.90	3662.01	447.93	306.48	204.32
Pb	0.94	0.86	1.07	0.84	0.73	0.68	0.67	0.60	0.72	0.59	0.33	1.40	1.02
Sr	591.91	67.65	101.47	50.74	50.74	93.01	372.06	370.20	380.10	219.85	710.30	541.18	693.38
V	15.10	48.54	62.73	221.11	165.83	186.24	149.19	150.50	140.81	47.38	69.84	78.34	55.41
Y	1.78	2.56	2.97	4.04	3.81	2.82	9.72	8.10	10.10	2.14	7.95	8.62	3.94
Zn	1478.20	176.74	192.81	128.54	168.71	176.74	152.64	150.40	152.17	361.52	232.98	160.67	208.88
Zr	1.59	2.72	3.38	3.61	3.64	2.68	7.83	8.10	8.42	10.01	8.68	9.93	10.04
Rb	1.00	0.52	0.87	0.66	0.24	0.35	0.87	0.66	0.95	0.64	0.91	0.70	1.06
Ga	3.18	6.12	5.78	7.18	7.14	6.52	11.02	12.30	13.28	4.80	10.66	14.47	11.34
Ba	7.67	18.69	16.14	11.24	18.43	6.18	11.78	13.10	14.42	14.04	6.33	45.28	10.27
As	3.11	6.94	4.86	6.36	5.85	4.59	7.95	6.90	7.47	4.94	5.59	7.61	4.72
Se	1.33	1.85	1.42	1.79	1.31	1.10	1.41	1.90	1.85	1.48	1.65	1.10	1.49
Br	1.77	2.37	2.28	2.44	2.96	2.05	2.66	2.10	1.98	2.11	1.83	3.06	2.29

antigorite occurs in two forms, one as reticulated fine fibers around the boundaries of olivine phenocrysts and the second form presents in the groundmass as fine colorless aggregates of fibrolamellar nature that gives anomalous first order interference colors and parallel extinction (Fig. 4e).

Orthopyroxene is represented by enstatite and found as phenocrysts exhibits schiller structure and partly alters to bastite along the grain boundaries. Clinopyroxene is represented by diopside and present as long prismatic phenocrysts show two perpendicular sets of cleavage with white to yellow interference colors, polysynthetic twinning, oblique extinction, and partly altered to clinochlore, tremolite, and actinolite around the borders of these phenocrysts (Fig. 4f). Iddingsite shows a high relief and lamellar structure. It occurs as partial alteration pseudomorphs after olivine phenocrysts during many stages of structural and chemical change (Fig. 4e). Clinochlore is found in few amounts as an alteration product of pyroxene minerals. It is pleochroics from yellowish green to pale green forming sheaf-like bundles (Fig. 4f). It shows faint cleavage in one direction and forms cumulate crystals with anomalous berlin blue interference colors. Tremolite occurs as fibrous crystals, up to 0.1 mm long, pseudomorphs after pyroxene. It is partly rimmed or replaced by clinopyroxene (diopside). It is commonly associated with antigorite and brucite in the groundmass (Fig. 4e). Brucite occurs in colorless, fine plates or scaly aggregates that appear fibrous associated with antigorite. It is show fair relief and parallel extinction (Fig. 4e).

Carbonate minerals occur as fine to medium grain aggregates or patches, colorless, euhedral and subhedral crystals. Occasionally, these carbonates occur as mature and immature granular aggregates formed as an alteration product of plagioclase crystals (Fig. 5a). Opaque minerals granules are quite abundant in these rocks and represented by magnetite and chrome spinel. The crystals covered by networks of black cracks are olivines. Small and big isotropic grains of dark brown and black chrome-spinel and magnetite are present and are also highly deformed. Magnetite forms anhedral to subhedral equant granules, up to 0.7 mm diameter distributed randomly throughout the rocks or ordered in streaks along the cracks if the olivine phenocrysts (Fig. 5b. It is frequently altered to hematite (martite). It is commonly enclosing fine grains of clinochlore.

Table 2

Rock	Serpentinized peridotites						Dunites			Olivine gabbro			
S. No.	Z_{23}	Z_{24}	Z_{25}	Z_{26}	Z_{27}	Z_{30}	M_4	M_5	M_7	M_3	M_8	M_{13}	M_{14}
Ag	3.52	5.17	4.98	5.57	7.25	4.09	6.86	7.10	8.50	5.02	5.57	6.81	5.86
Cd	1.76	2.16	1.64	1.66	3.01	0.72	2.92	3.50	2.99	1.93	2.32	3.66	2.10
Sb	3.29	4.02	3.59	3.50	3.10	3.24	4.04	4.15	4.34	4.16	4.32	2.54	2.41
Te	3.36	–	2.41	0.30	–	2.30	–	–	–	2.28	0.68	–	0.01
I	10.21	15.98	14.35	13.41	14.77	14.73	16.25	15.79	15.53	14.79	15.37	20.21	16.01
Cs	8.28	–	0.90	–	–	–	–	–	–	–	–	–	–
Hf	3.74	–	–	–	0.02	–	–	–	–	–	–	–	–
W	5.02	14.84	13.71	8.23	24.27	5.25	6.01	6.75	7.00	6.75	3.75	66.30	15.86
Tl	4.05	5.18	5.06	5.63	5.50	3.42	5.78	4.50	6.50	3.31	4.69	6.04	3.74
Bi	–	0.30	–	0.01	1.48	0.01	–	–	–	–	–	1.32	0.68
Th	–	–	–	–	–	–	–	–	–	–	–	–	–
Ge	–	–	–	–	–	–	–	–	–	–	–	–	–
Sn	–	–	–	–	–	–	–	–	–	–	–	–	–
Hg	–	–	–	–	–	–	–	–	–	–	–	–	–
REE (ppm)													
La	2.70	5.78	6.20	–	–	–	19.87	20.80	22.40	10.91	–	2.09	3.72
Ce	–	1.13	–	–	8.32	–	–	–	–	15.99	0.76	–	3.28
Nd	–	4.43	–	–	2.57	0.97	–	–	–	3.23	–	–	8.56
Sm	5.46	–	–	–	2.63	–	4.78	5.30	3.70	10.29	–	–	–
Yb	–	–	–	–	–	–	–	–	–	–	–	–	–
Pr	–	–	–	–	–	–	–	–	–	–	–	–	–
Eu	–	–	–	–	–	–	–	–	–	–	–	–	–
Gd	–	–	–	–	–	–	–	–	–	–	–	–	–
Tb	–	–	–	–	–	–	–	–	–	–	–	–	–
Dy	–	–	–	–	–	–	–	–	–	–	–	–	–
Ho	–	–	–	–	–	–	–	–	–	–	–	–	–
Er	–	–	–	–	–	–	–	–	–	–	–	–	–
Tm	–	–	–	–	–	–	–	–	–	–	–	–	–
Lu	–	–	–	–	–	–	–	–	–	–	–	–	–

Ferriferous brucite or magnetite, or both, may be associated with the serpentine (antigorite).

Olivine gabbro are coarse-grained, well-developed ophitic, subophitic, and symplectite textures. They are composed principally of plagioclase, pyroxene, and olivine (Fig. 5c-f). Sometimes, talc and iddingsite may be present as an alteration product of olivine. Occasionally hornblende may be present. Titaniferous magnetite, chrome spinel, and orthopyroxene are the main accessories. These olivine gabbro exhibit symplectite texture (Fig. 5c): symplectite of opaque and orthopyroxene. There are arrows indicate individual worm-like opaque bodies present in the orthopyroxene. Opaque minerals (Titaniferous magnetite and chrome spinel) and small crystals of orthopyroxene are intimately intergrown in a vermicular fashion (wormlike) in the spaces between plagioclase, augite, and other opaque minerals. Bleb-like intergrowth of augite in orthopyroxene is found in the olivine gabbro (Fig. 5d). In these rocks blebs of augite are embedded in an orthopyroxene host, forming an 'emulsion-like' texture. Though the blebs are irregular in shape they have a common elongation

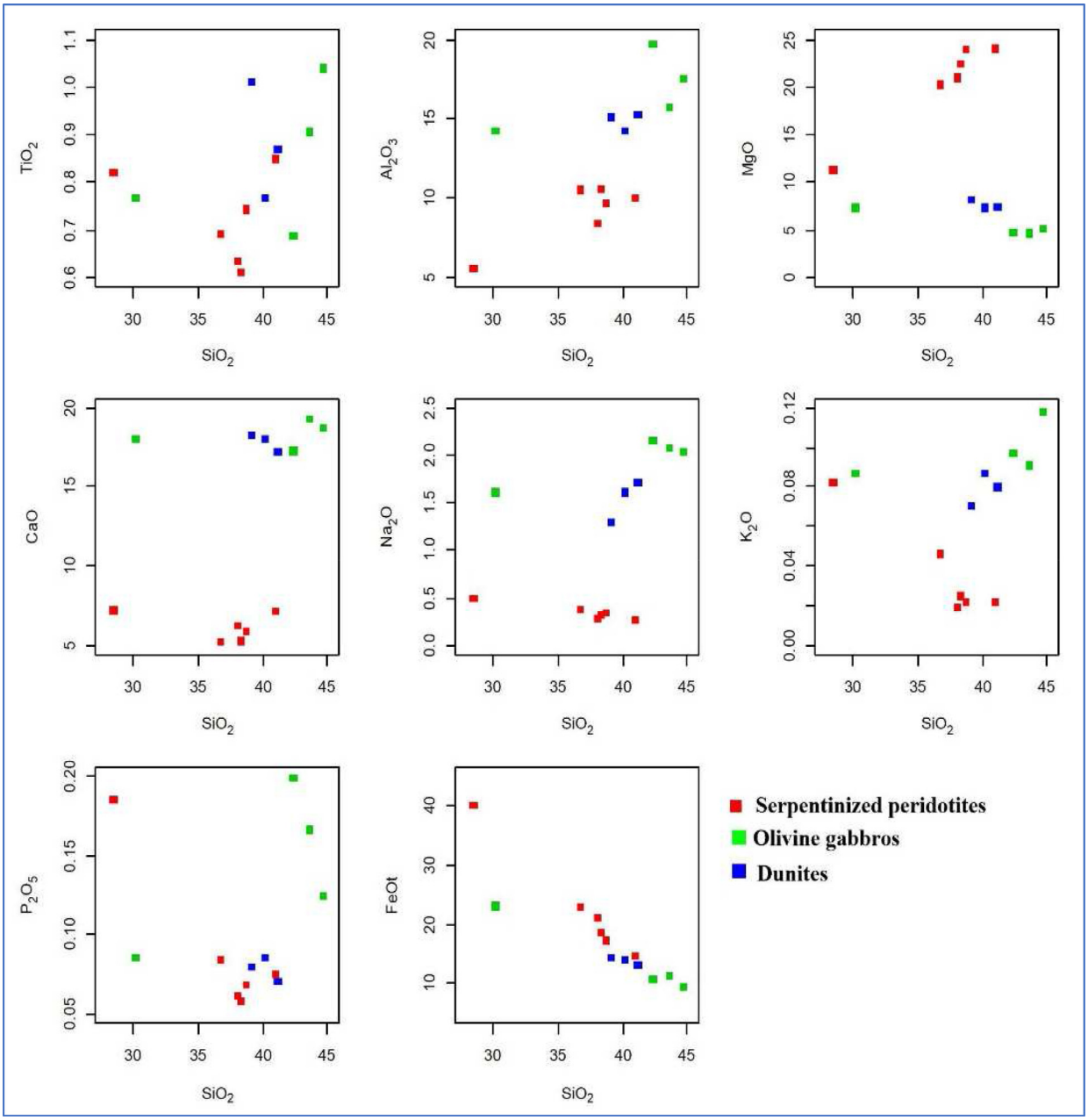

Fig. 6. Variation of major oxides in the investigated ultramafic-mafic intrusive complex.

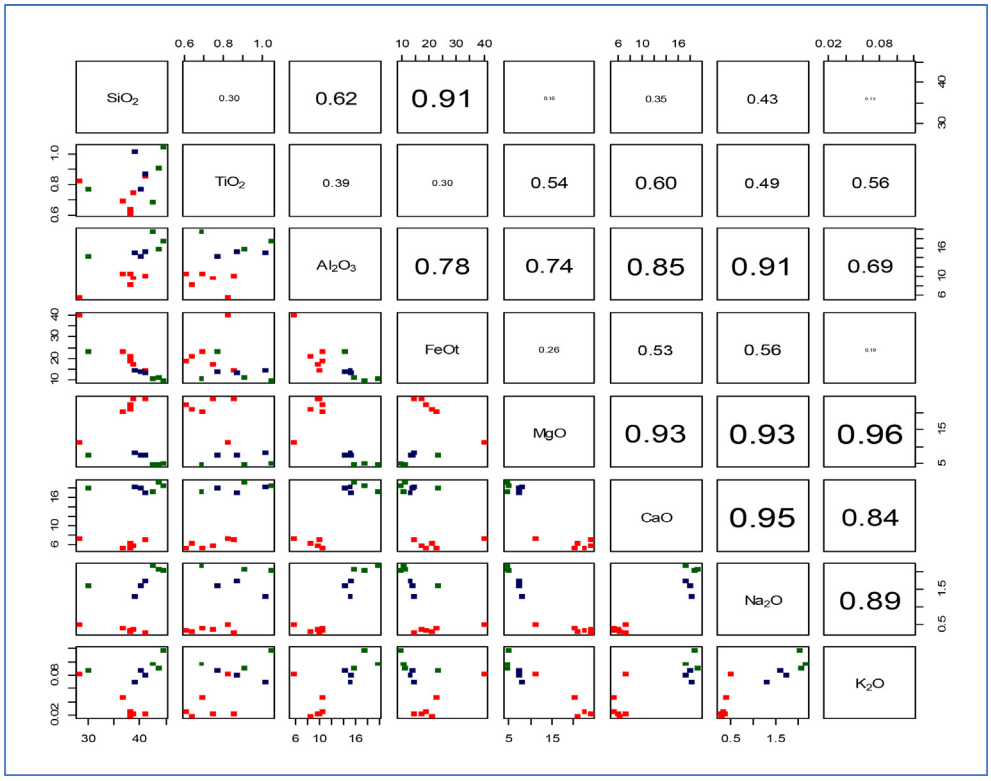

Fig. 7. Correlation diagram of major oxides in the investigated ultramafic-mafic intrusive complex.

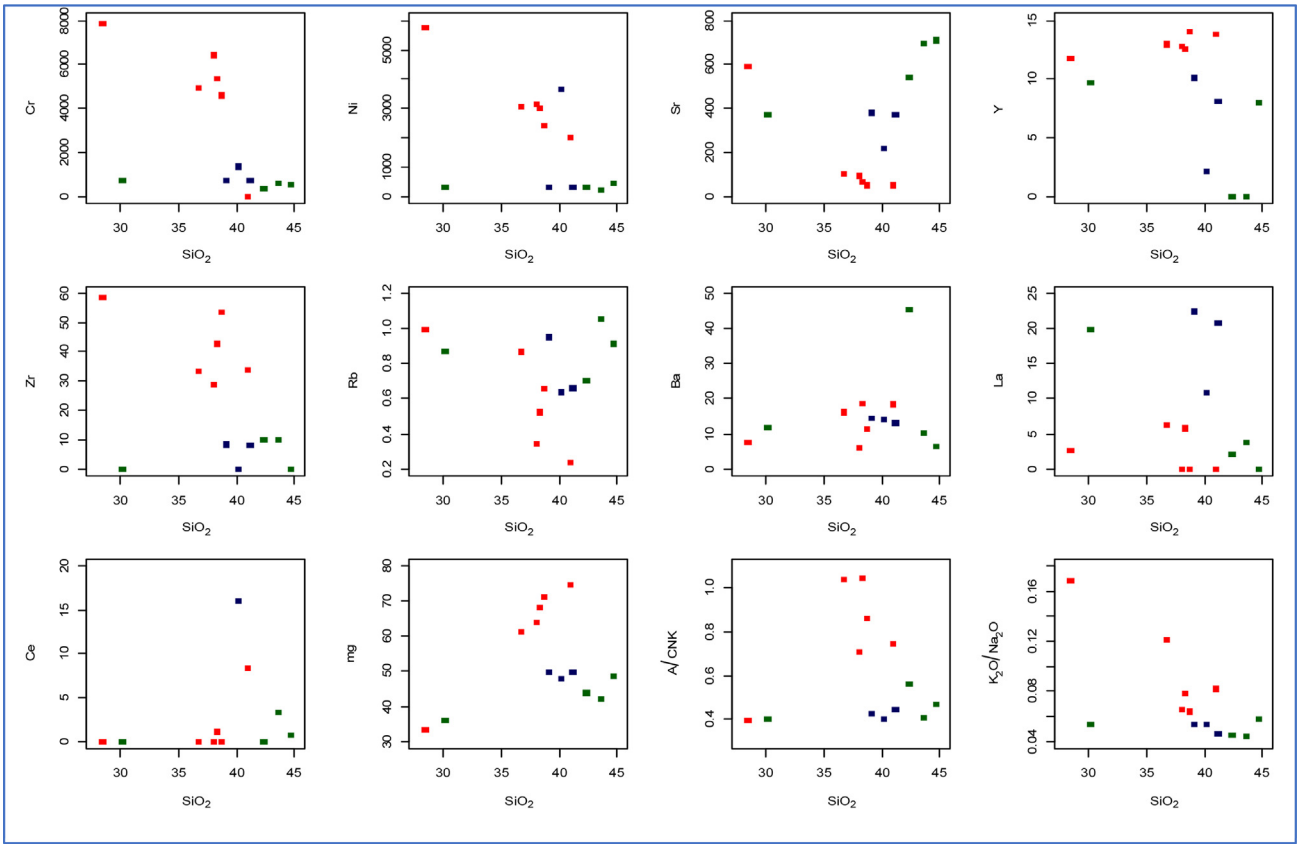

Fig. 8. Variation of trace elements of the investigated ultramafic-mafic intrusive complex.

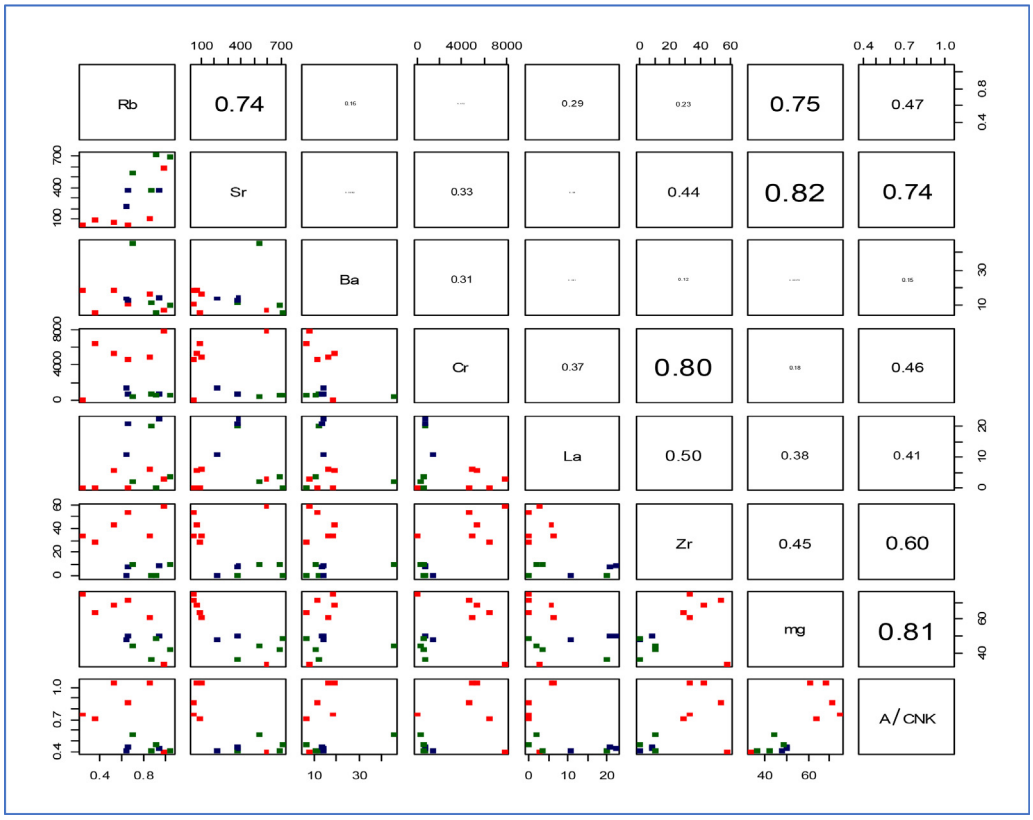

Fig. 9. Correlation diagram of trace elements of the investigated ultramafic-mafic intrusive complex.

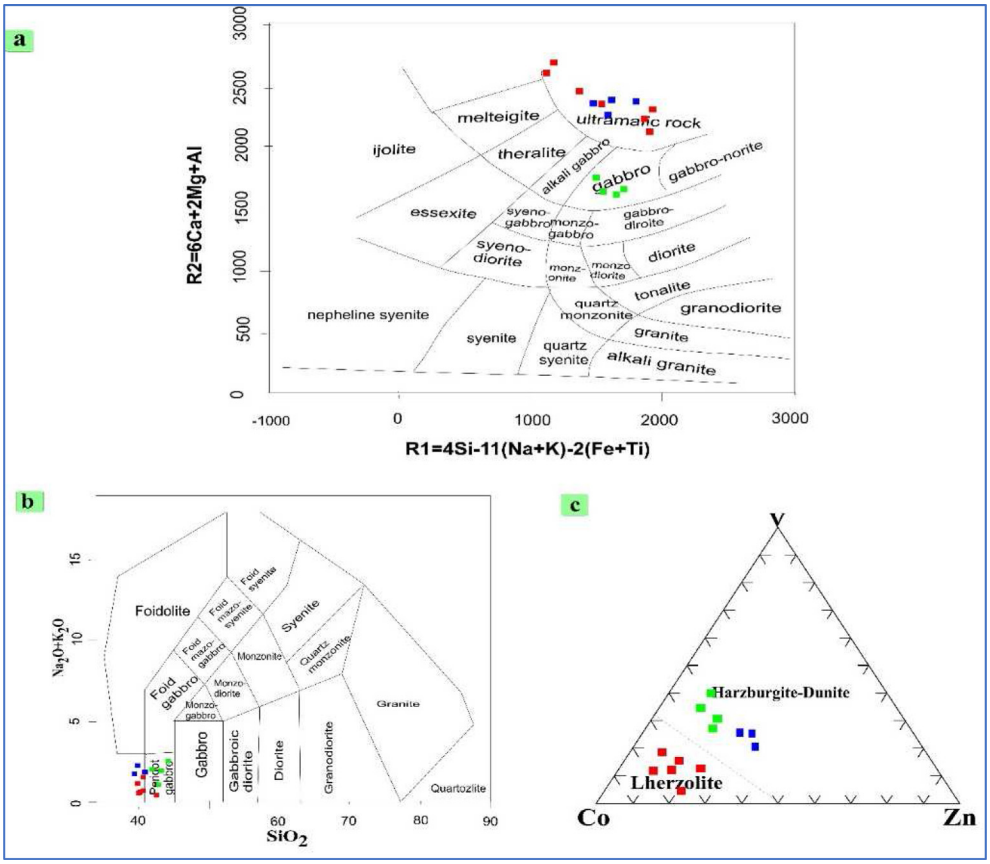

Fig. 10. (a) R1-R2 plot binary diagram for the ultramafic-mafic intrusive complex [13]. (b) ($Na_2O + K_2O$) versus SiO_2 binary diagram [14]. (c) V−Co−Zn ternary diagram [15].

direction and the same optical orientation. Plagioclase (anorthite to bytownite) occurs as coarse-grained, subhedral tabular crystals with averages about 0.5 mm in length and 0.3 mm in width (Fig. 5c). It is frequently well twinned, percline, and Carlsbad twinning (Fig. 5d).

Pyroxene (titanaugite) is found as coarse-grained, subhedral long prismatic crystals, which characterized by high interference colors (Fig. 5c). Occasionally, hypersthene crystals commonly enclose lamellae of resolved diopside. Olivine present as coarse-grained, equidimensional crystals, high relief of irregular fractures and strong interference colors. Olivine is partially replaced by reddish-brown iron oxides along its microfractures; this pseudomorphs alteration is recognized by iddingsite (Fig. 5e). Opaque minerals are found as coarse-grained, euhedral crystals dispersed throughout the mineral constituents and represented by magnetite and chrome spinel. Also, it occurs as medium grains arranged along the micro-cracks and cleavage planes of minerals (Fig. 5f).

4.2. Geochemical characteristics

13 samples of ultramafic-mafic intrusive complex represented by peridotites (6 samples), dunites (3 samples) and olivine gabbro (4 samples) were analyzed to determine their geochemical characteristics and origin (Tables 1 and 2). The results of major oxides, trace elements and rare earth elements of ultramafic-mafic intrusive complex are given in Tables 1 and 2 The serpentinized peridotites reveals quite variation in the major oxides as follows: SiO_2 is varies from 28.09 to 40.22%, MgO ranges from 11.31 to 24.08%, TiO_2 ranges from 0.21 to 0.42%), Al_2O_3 ranges from 5.57 to 10.56%, $Fe_2O_3^{tot}$ varies from 16.32 to 44.63%, CaO ranges from 5.22 to 7.2% with an average 6.14%, the average concentrations of total alkali $Na_2O + K_2O$ are 0.19%, average of MnO are 0.09% and average of P_2O_5 are 0.33%. The study serpentinized peridotites shows also variation in concentration of the trace elements as follow: Cr content are high and ranges from 7861 to 4590 ppm with an average 5645 ppm, Ni with an average 3908 ppm, Co

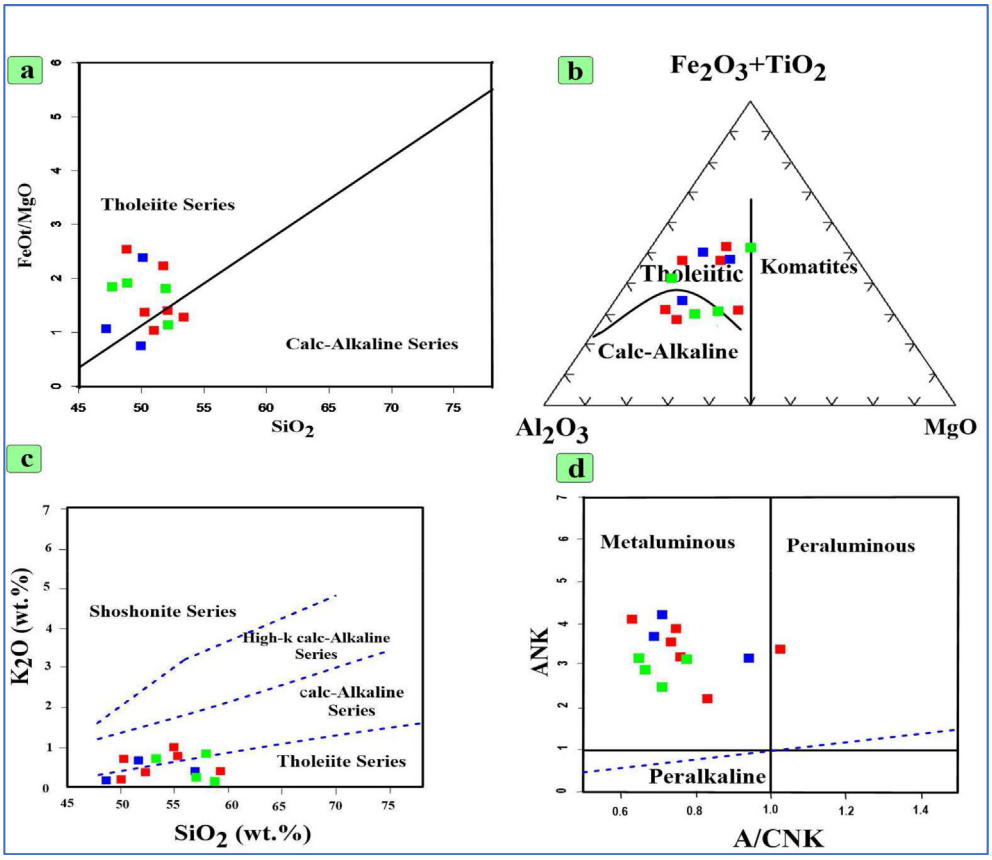

Fig. 11. (a) FeOt/MgO versus SiO_2 diagram of [16] for the ultramafic-mafic intrusive complex. (b) (Al_2O_3-(Fe_2O_3t + TiO_2) versus (MgO) ternary diagram of [17]. (c) SiO_2 versus K_2O binary diagram of [18]. (d) ANK versus ACNK variation diagram of [19].

with an average 643.60 ppm, V with an average 116.59 ppm, Sr with an average 159.25 ppm, Cu with an average 165.86 ppm, Zn with an average 386.96 ppm, with less frequently amounts of Zr with an average 2.94 ppm, Sc with an average 8.97 ppm, and Y with an average 3 ppm (Table 1).

The dunites have narrow variations in the major oxides. The SiO_2 content ranges from 39.12 to 41.19%, MgO ranges from 7.3 to 8.1%, TiO_2 ranges from 0.77 to 1.01%, Al_2O_3 ranges from 14.26 to 15.24%, $Fe_2O_3^{tot}$ ranges from 14.71 to 16.1%, CaO content ranges from 17.2 to 18.3% with an average 17.8%, the average concentrations of total alkali ($Na_2O + K_2O$) is 0.81%, the average concentrations of MnO and P_2O_5 are 0.23% and 0.08% respectively. Dunites are distinctly enriched in Cr content with an average 712.42 ppm, Ni with an average 299.91 ppm, Co with an average 289.77 ppm, V with an average 146.83 ppm, Sr with an average 374.12 ppm, Cu with an average 346.64 ppm, Zn with an average 151.74 ppm, Sc with an average 43.08 ppm, with less frequently amounts of Zr content with an average 8.12 ppm, Pb with an average 0.66 ppm, and Y content with an average 9.31 ppm (Table 1).

The olivine gabbro have wide variations in SiO_2 content and ranges from 31.16 to 39.37%, MgO ranges from 4.72 to 17.43%, TiO_2 ranges from 0.46 to 1.04%, Al_2O_3 ranges from 5.82 to 19.7%, $Fe_2O_3^{tot}$ ranges from 14.94 to 36.28%, CaO ranges from 6.35 to 19.32% with an average 6.14%, the average concentrations of total alkali ($Na_2O + K_2O$) is 0.90%, the average contents of MnO and P_2O_5 are 0.09% and 0.55%, respectively. The silica content depleted with increase $Fe_2O_3^{tot}$. Olivine gabbro enriched in Ni content with an average 1155.19 ppm, Cr with an average 709.86 ppm, Co with an average 464.03 ppm, Sr with an average 541.18 ppm, Cu with an average 293.58 ppm, and Zn with an average 241.01 ppm, less frequently amounts of Zr with an average 9.67 ppm, Sc with an average 19.45 ppm, V with an average 62.74 ppm, and Y with an average 5.66 ppm (Table 1).

The SiO_2 contents of the present serpentinized peridotites, dunites, and olivine gabbro are plotted against some major oxides and trace elements (Figs. 6–9). The relationship between SiO_2 and major oxides exhibits a negative correlation with Fe_2O_3 and MgO (decrease with increasing SiO_2 contents). Meanwhile, the Al_2O_3, CaO, and Na_2O show a

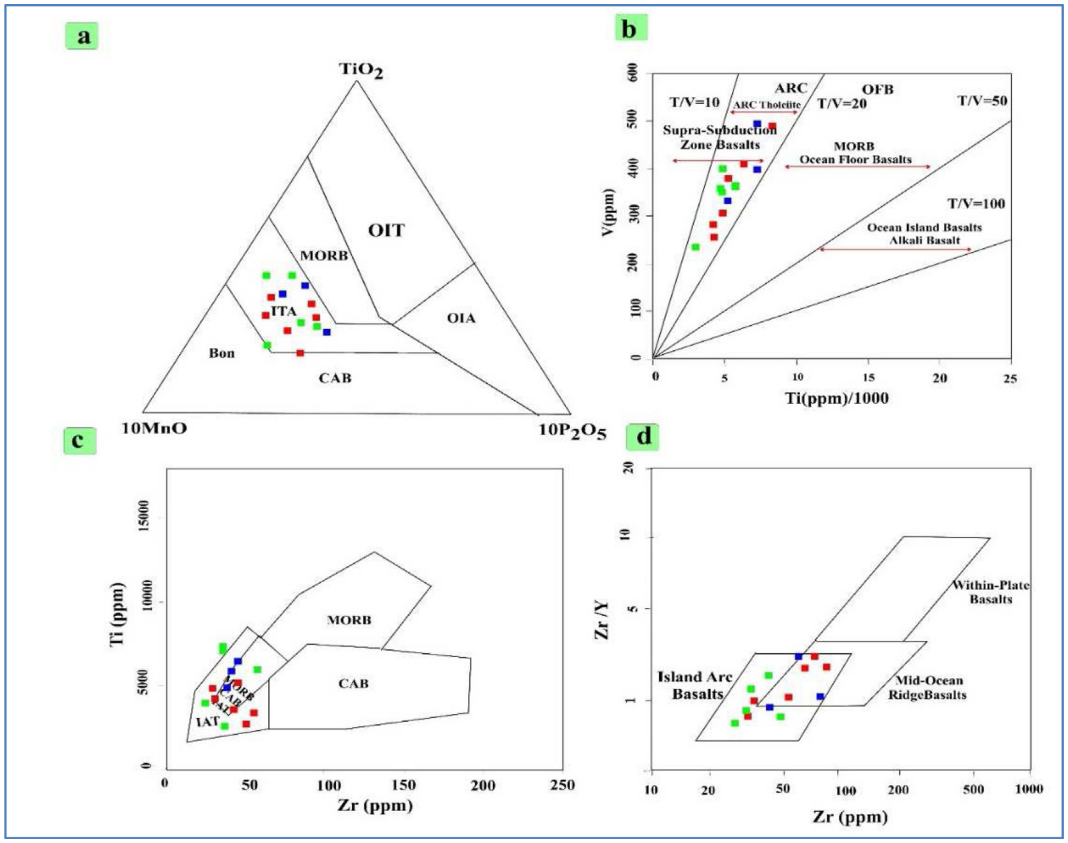

Fig. 12. (a) MnO–TiO_2–P_2O_5 ternary diagram of [20] for the ultramafic-mafic intrusive complex. (b) Ti–V binary diagram of [21]. (c) Zr–Ti binary diagram of [22]. (d) Zr/Y -Zr binary diagram of [23].

positive correlation (increase with increasing SiO_2 contents; Figs. 6 and 7). The relationship between SiO_2 and trace elements exhibits a negative correlation with Ni, Cr, and Sr. Meanwhile, the Y, Zr, La, and Rb, show a positive correlation (Figs. 8 and 9).

4.2.1. Geochemical classification and nomenclature

According to R1 versus R2 binary diagram (Fig. 10a) of De La Roche [13], the samples of ultramafic-mafic intrusive complex were plot on the ultramafic rocks and gabbro fields. On the $Na_2O + K_2O$ versus SiO_2 binary diagram of Middlemost [14], the samples of ultramafic-mafic intrusive complex were plot on gabbroic field (Fig. 10b). On this diagram, the silica and total alkalis are depleted due to high mineralization of iron oxides, which explains why some samples are plotted outside of the field of peridotite - gabbro (Fig. 10b). On ternary diagram V−Co−Zn of Gulacar and Delaloye [15], all samples of serpentinized peridotites plotted in the lherzolite field while dunites and olivine gabbro are plotted in harzburgite-dunite field (Fig. 10c).

4.2.2. Magma type and tectonic setting

The magma type of the studied ultramafic-mafic intrusive complex can be identified by the following diagrams. According to the FeOt/MgO versus SiO_2 binary diagram, all samples plot in the tholeiitic and calc-alkaline fields (Fig. 11a) the dividing line is after Miyashiro [16]. The $(Fe_2O_3 + TiO_2) - Al_2O_3 - MgO$ ternary diagram of Jensen [17] illustrates the nature of primary magma of the ultramafic-mafic intrusive complex. On this diagram, the studied samples plot in the tholeiitic to calc-alkaline fields (Fig. 11b). According to SiO_2 versus K_2O binary diagram of Peccerillo and Taylor [18], the ultramafic-mafic intrusive complex plot in the tholeiitic to calc-alkaline fields (Fig. 11c) Maniar and Piccoli [19]. used the $Al_2O_3/(CaO + Na_2O + K_2O)$ [A/CNK] versus

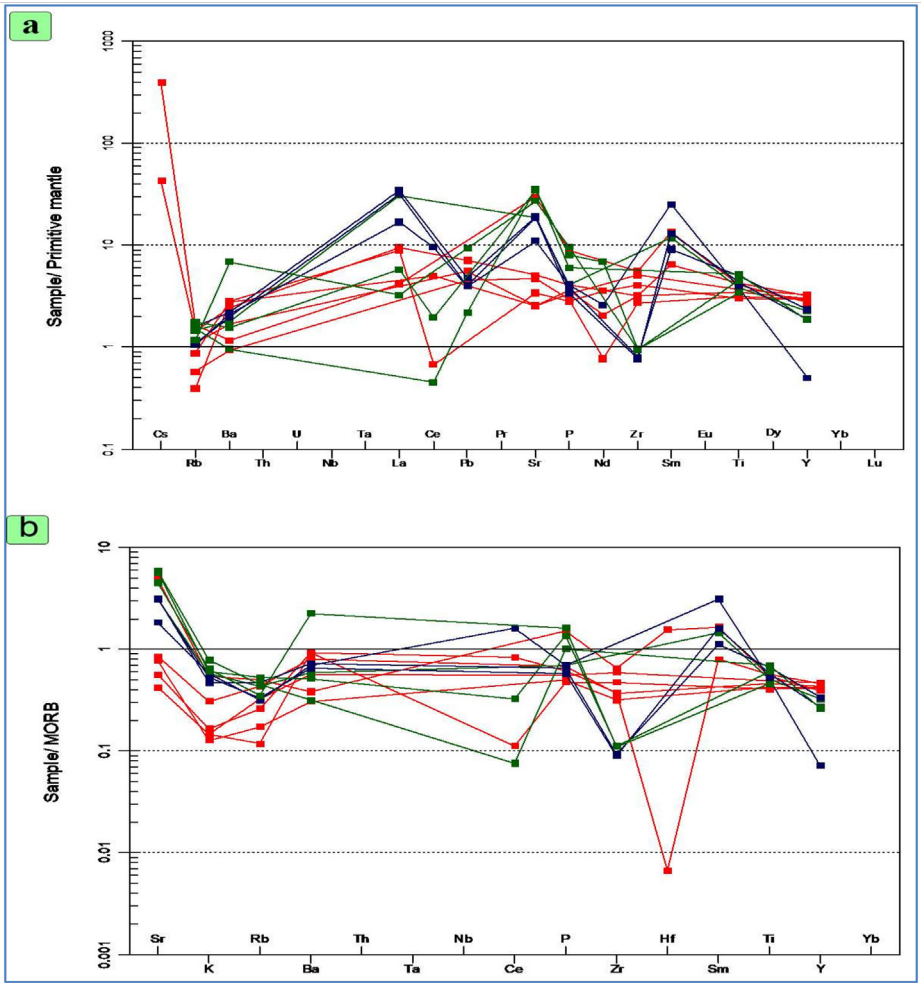

Fig. 13. (a & b) MORB and primitive mantle-normalized trace element spider diagrams for the ultramafic-mafic intrusive complex. MORB and primitive mantle normalization values are from [22,24] respectively.

$Al_2O_3/(Na_2O + K_2O)$ [A/NK] variation diagram to identify the different types of magmatic rocks such as peraluminous, metaluminous and peralkaline. The analyzed samples plot in the metaluminous except one sample plots in peraluminous field (Fig. 11d).

The tectonic setting of the studied ultramafic-mafic intrusive complex can be deduced from the following relationships. In the $MnO-TiO_2-P_2O_5$ ternary diagram of Mullen [20], the ultramafic-mafic intrusive complex plot in the mid-ocean ridge basalts (MORB) but some samples plotting in the island arc tholeiites (IAT) field (Fig. 12a). On the Ti versus V binary diagram of Shervais [21], the ultramafic-mafic intrusive complexes plot in the mid-ocean ridge basalts (MORB; Fig. 12b). According to Zr−Ti binary diagram of Pearce [22], the ultramafic-mafic intrusive complex plot within island arc tholeiitic (IAT) and mid-ocean ridge basalt (MORB) field (Fig. 12c). According to Zr/Y -Zr binary diagram of Pearce and Norry [23], the analyzed samples plot in the island arc basalt and mid-ocean ridge basalt fields (Fig. 12d). Relative to the primitive mantle of the ultramafic-mafic intrusive complex is enriched in Rb, Ba, U, Th, P, and other large ion lithophile elements (LILE), but depleted in Ce, Zr, Hf, Sm, Ti, Y, Yb, and high field strength elements (HFSE); Shervais [21]. On MORB normalized spider diagrams the samples are enriched in Sr, Sm, Zr, P, and Cs but depleted in Yb, Y, Ti, Nb, Th, and Ta Taylor and McLennan [24] (Fig. 13a & b.

4.3. Mineralization

4.3.1. Ore microscopic investigation

A detailed study of the mode of occurrence of both oxide minerals and gangue minerals were carried out on the collected samples of Wadi Zayatit and Wadi Mikbi ultramafic-mafic intrusive complex. The examined thin-polished sections exhibit that they contain ilmenite, chromite, titanomagnetite, and magnesioferrite. Chromite occurs as euhedral

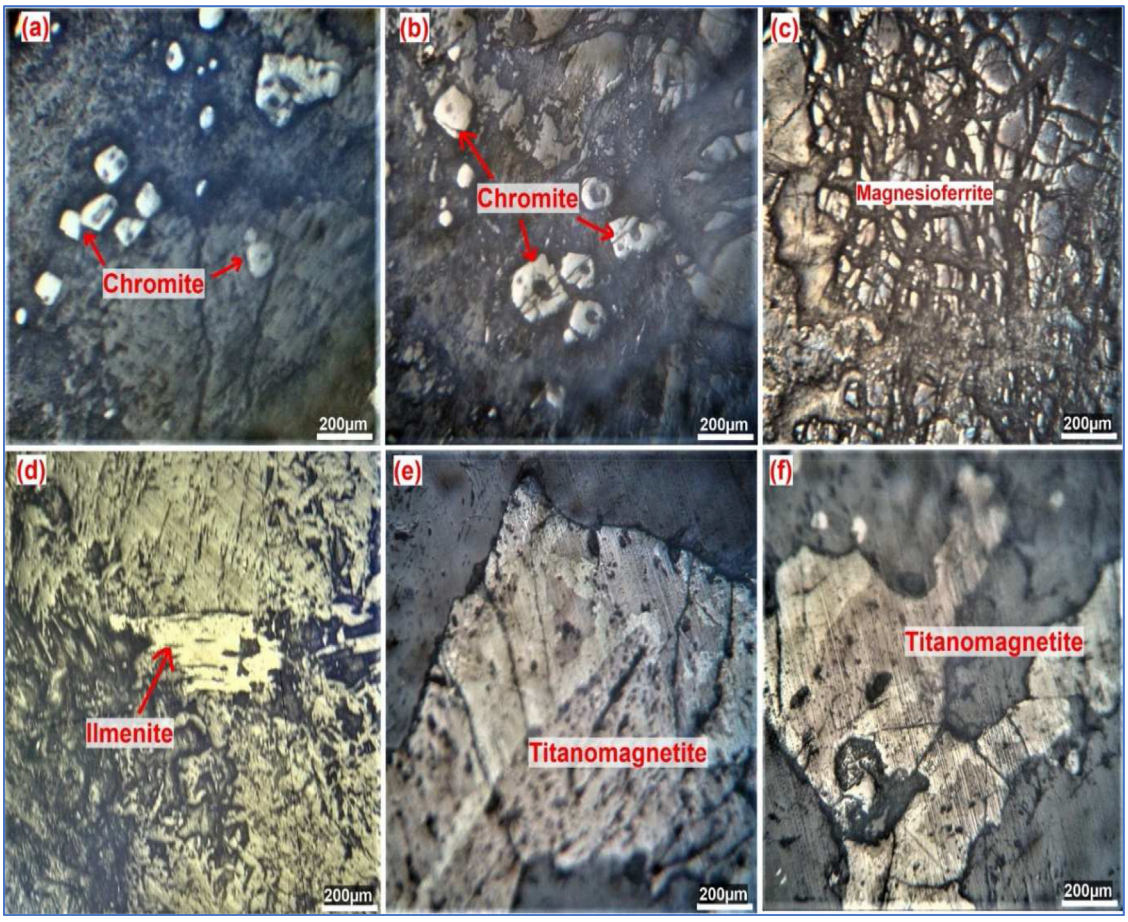

Fig. 14. Photomicrographs showing (a) Euhedral crystals of chromite within peridotites. (b) Euhedral crystals of chromite within peridotites. (c) Disseminated grains and anhedral magnesioferrite crystals within peridotites. (d) Euhedral crystal of ilmenite within olivine gabbros. (e) Coarse grains of titanomagnetite crystals within olivine gabbros. (f) Subhedral titanomagnetite crystals within olivine gabbros.

crystals and zoned crystals of grey color and dark brown to brown internal reflection. It occurs as irregular to euhedral fractured crystals with silicate minerals filling the cracks (Fig. 14a). Chromite represents the most common opaque mineral encountered in Wadi Zayatit peridotite samples (Fig. 14b). Magnesioferrite occurs as disseminated euhedral to subhedral grains, grey in color, and elongated granules crystals (Fig. 14c). Magnesioferrite crystals included within Wadi Zayatit peridotites (Fig. 14c). Ilmenite found as subhedral elongated crystals of tabular like shape. Usually, it occurs as plates, separate grains, and as whitish black and grey small bodies. Ilmenite hosted in Wadi Mikbi olivine gabbro (Fig. 14d). Ilmenite altered to titanomagnetite that found in Wadi Mikbi olivine gabbro. Titanomagnetite appears as coarse-grained, subhedral, irregular crystals and exsolution of fine network intergrowth of titanomagnetite within magnetite and ilmenite crystals (Fig. 14e). Titanomagnetite is formed when magnetite contains lamellar exsolution of ilmenite. Titanomagnetite crystals observe in Wadi Mikbi olivine gabbro (Fig. 14f). Ilmenite crystals altered completely to titanomagnetite within the Wadi Mikbi olivine gabbro. In olivine gabbro, it appears as elongated granules with fine needles of ilmenite that forming fine network intergrowth (Fig. 14e).

4.3.2. Mineralogy of the studied rocks (XRD and SEM/EDX investigations)

The identified minerals by XRD technique are chromite, ilmenite, quartz, plagioclase clinochlore minerals encountered in peridotites and olivine gabbro of the studied ultramafic-mafic intrusive complex (Fig. 15a & b). The mineralogy of peridotites is composed essentially of chromite and clinochlore (Fig. 15a). The mineralogy of olivine gabbro is composed chiefly of ilmenite, quartz, plagioclase, and pyroxene (Fig. 15b). EDX analyses of small thin polished section from Wadi Zayatit and Wadi Mikbi ultramafic-mafic intrusive complex proved the presence of the chromite and ilmenite. EDX analyses of chromite crystals spotted within the dunites (Fig. 16a). These microchemical analyses display high peaks of Fe (60.10%), Cr (24.52%), O (15.62%)

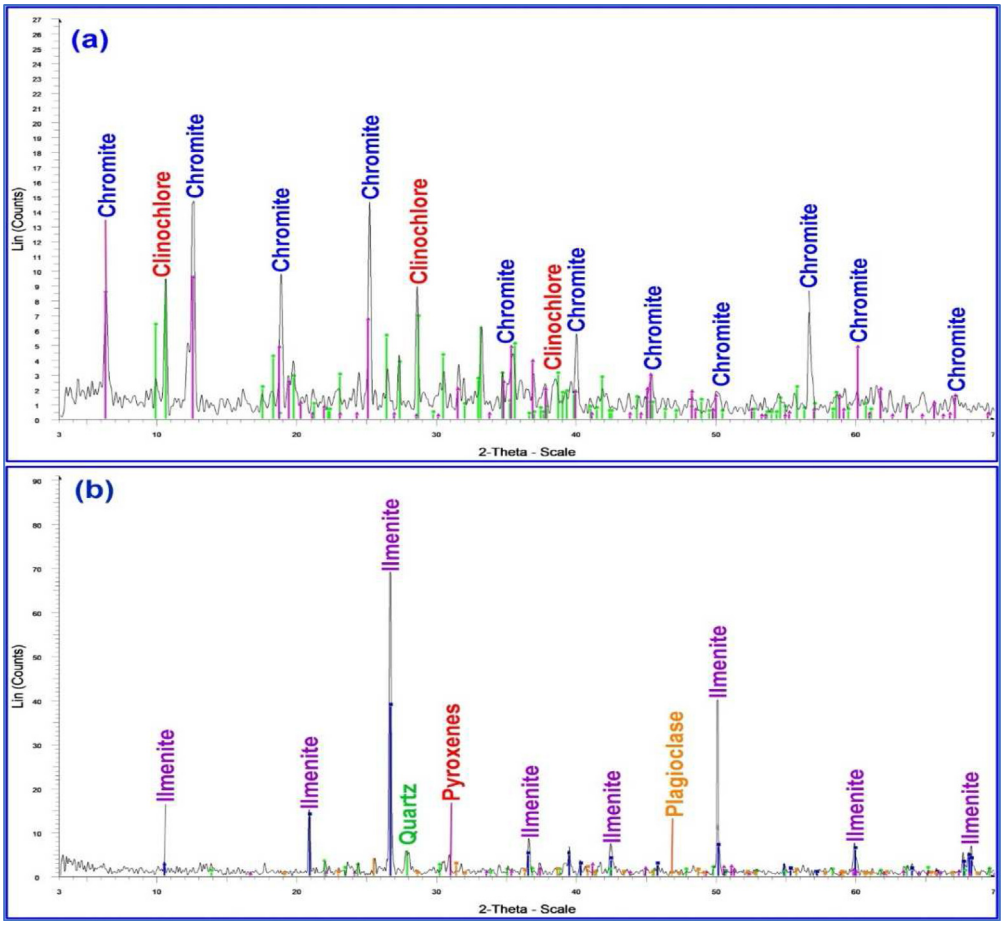

Fig. 15. X-ray diffractograms of the heavy fractions of display chromite, ilmenite, quartz, plagioclase, pyroxene and clinochlore. a) Peridotites, b) Olivine gabbros.

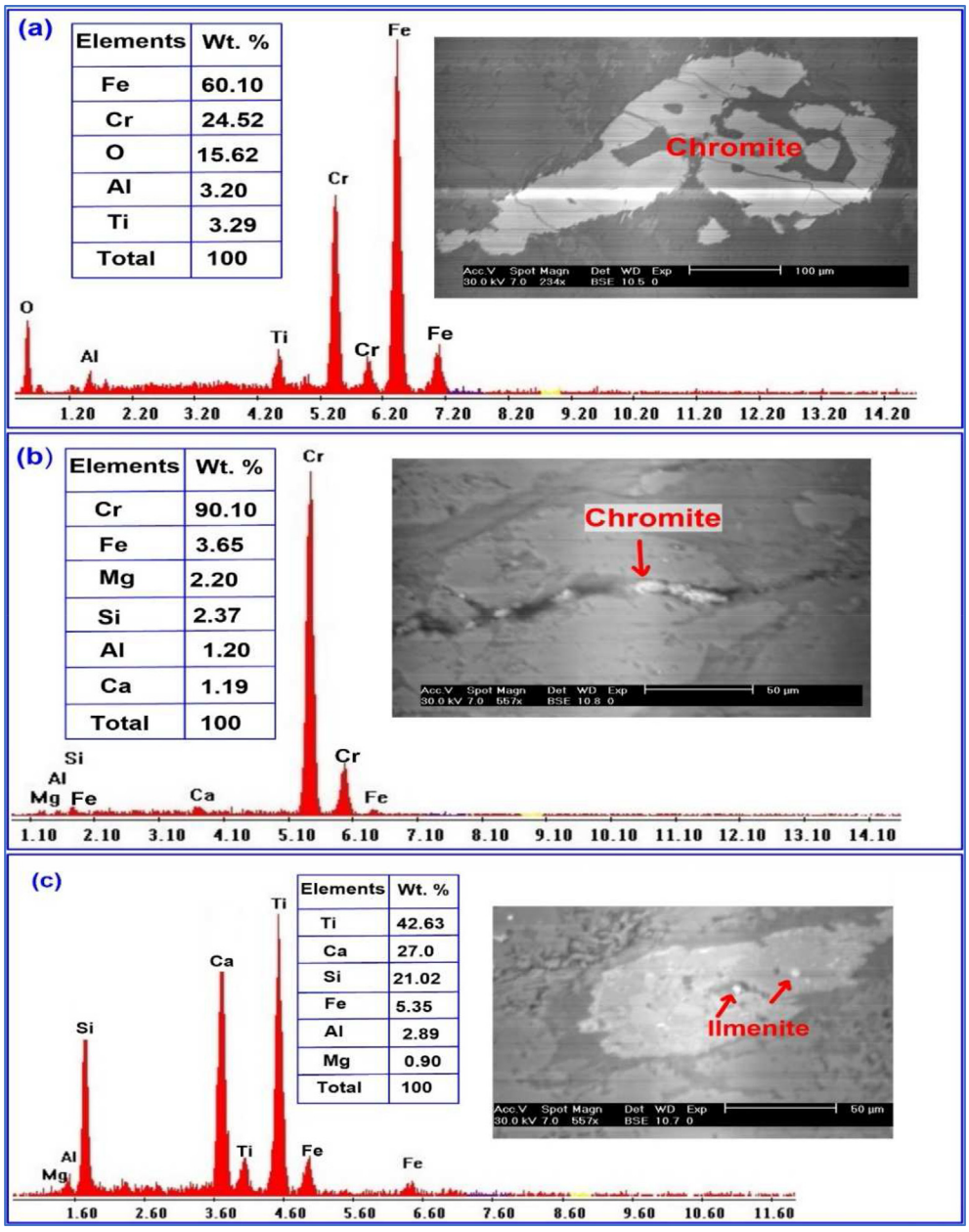

Fig. 16. BSE image and EDX spot analysis showing: (a) Chromite crystals-bearing dunites. (b) Chromite crystals-bearing Peridotites. (c) Ilmenite crystals-bearing olivine gabbros.

and small peaks from Al (3.20%), and Ti (3.29%) found in the dunites (Fig. 16a). The analysis of chromite crystals within the peridotite displays high peaks of Cr (90.10%), Fe (3.65%) and small peaks from Mg (2.20%), Si (2.37%), Al (1.20%), and Ca (1.19%) (Fig. 16b). EDX analyses of fine granular ilmenite crystals are disseminated in olivine gabbro (Fig. 16c). The X-ray spectrum profile obtained from EDX microchemical analysis of ilmenite found in the olivine gabbro displays high peaks of Ti (42.63%), Ca (27.0%), Si (21.02%), Fe (5.35%), Al (2.89%), and Mg (0.90%) (Fig. 16c).

5. Conclusions

The present work deals with the field geology, petrography, geochemistry and mineralization of Wadi Zayatit and Wadi Mikbi ultramafic-mafic intrusive complex, South Eastern Desert, Egypt. These Alaskan type ultramafic-mafic intrusive complexes occupy the central northern part of Wadi Mikbi and south part of Wadi Zayatit district.

(1) The basement rocks of Wadi Zayatit and Wadi Mikbi ultramafic-mafic intrusive complex are the

main constituents of the dunites, peridotites, and gabbro.

(2) These rocks are coarse-grained, dark greyish to whitish grey in color. These rocks are massive with lustric features, and slightly deformed with low to moderate relief. The commonest of the accessory constituents is an oxide ore mineral of some kinds, the most frequent one is chromite and titanomagnetite.

(3) Petrographically, the ultramafic-mafic intrusive complex is represented by dunites, serpentinized peridotites, and olivine gabbro.

(4) These rocks are of a layered igneous complex, markedly heterogeneous nature in its outcrop, and coarse-to very coarse-grained, and also exhibit pegmatoidal texture.

(5) Dunites are almost pure olivine rocks and consist of masses of strained and deformed closely knit olivine anhedral crystals.

(6) Peridotite consists essentially of phenocrysts of olivine (forsterite) and two kinds of pyroxene (enstatite and diopside) in a groundmass, which commonly contains serpentine (antigorite), chrome spinel, magnetite, brucite, clinochlore, and immature carbonate minerals. Peridotites are containing both orthopyroxene (enstatite) and clinopyroxene (diopside).

(7) Olivine gabbro are coarse-grained, well-developed ophitic, subophitic, and symplectite textures. They are composed principally of plagioclase, pyroxene, and olivine. The commonest of the accessory constituents is an oxide ore mineral of some kinds, the most frequent one is chromite and titanomagnetite.

(8) Geochemically, the study ultramafic-mafic intrusive complex originated from metaluminous and tholeiitic to calc-alkaline magma. The study ultramafic-mafic intrusive complex developed in the island arcs and mid-ocean ridge basalt environments.

(9) Based on the mineralogical studies using ore microscope, XRD, and SEM of representative mineral deposits samples collected from Wadi Zayatit and Wadi Mikbi ultramafic-mafic intrusive complexes, the main ore deposits comprise ilmenite, chromite, titanomagnetite and magnesioferrite.

Conflict of Interest

None declared.

Acknowledgements

The authors deeply thank Geology Department, Faculty of Science, Al-Azhar University.

References

[1] Abdallah SE, Shehata A, Obeid MA. Geochemistry of an Alaskan-type mafic-ultramafic complex in Eastern Desert, Egypt: new insights and constraints on the Neoproterozoic island arc magmatism. Geosci Front 2019;10:941–55.

[2] Abd El-Wahed M, Kamh S, Ashmawy M, Shebl A. Transpressive structures in the Ghadir shear belt, Eastern Desert, Egypt: evidence for partitioning of oblique convergence in the arabian nubian Shield during Gondwana agglutination. Acta Geol. Sin. - English Ed 2019;93:1614–46.

[3] Hamimi Z, Hagag W, Fritz H, Baggazi H, Kamh S, Hamimi Z, et al. The tectonic map and structural provinces of the late neoproterozoic Egyptian nubian Shield. In: Implications for crustal growth of the arabian–nubian Shield (east african orogen). vol. 10; 2022.

[4] Kotb H, Khaffagy MB, Swifi BM. Geochemistry and petrochemistry of Egyptian titaniferous gabbro. Ann Geol Surv Egypt 1980:627–50.

[5] Madbouly MI. Comparative study on petrology and geochemistry of some mafic-ultramafic intrusion of the South Eastern Desert and Sinai, Egypt. Egypt: Ph.D., Fac. Sci., Cairo Univ.; 2000.

[6] Helmy HM, El Mahallawi MM. Gabbro akarem maficeultramafic complex, Eastern Desert, Egypt: a late precambrian analogue of alaskanetype complexes. Mineral Petrol 2003;77: 85–108.

[7] Helmy HM, Yoshikawa M, Shibata T, Arai S, Kagami H. Sm-Nd dating and petrology of Abu Hamamid intrusion, Eastern Desert, Egypt: a case of Neoproterozoic Alaskan-type complex in a back-arc setting. Precambrian Res 2015; 258:234–46.

[8] Abdel Halim A, Helmy HM, Abdel-Rahman YM, Shibata T, El-Mahallawi MM, Yoshikawa M, et al. Petrology of the Motaghairat mafic-ultramafic complex, Eastern Desert, Egypt: a high-Mg post-collisional extension-related layered intrusion. J Asian Earth Sci 2016;116:164–80.

[9] Abdel-Karim AM, Ali SH, Helmy HM, El-Shafei SHA. Forearc setting of the Gerf ophiolite, Eastern Desert, Egypt: evidence from mineral chemistry and geochemistry of ultramafites. Lithos 2016;263:52–65.

[10] Pearce JA, Stern DW. Origin of back-arc basin margins: trace element and isotope perspectives. Geophys Monogr 2006; 166:63–86.

[11] Batanova VC, Pertsev AN, Kamenetsky VS, Ariskin AA, Mochalov AG, Sobolev AV. Crustal evolution of islandearc ultramafic magma: galmoenan pyroxeniteedunite plutonic complex, Koryak, Highland (Far East Russia). J Petrol 2005; 46:1345–66.

[12] Teng XM, Yang QY, Santosh M. Devonian magmatism associated with arccontinent collision in the northern North China Craton: evidence from the Longwangmiao ultramafic intrusion in the Damiao area. J Asian Earth Sci 2015;113:626–43.

[13] De La Roche H, Leterrier J, Grandclaude P, Marchal M. A classification of volcanic and plutonic rocks using R1 R2-diagram and major-element analyses its relations with current nomenclature. Chem Geol 1980;29:183–210.

[14] Middlemost EAK. Naming materials in the magma/igneous rock system. Earth Sci Rev 1994;37:215–24.

[15] Gülaçar OF, Delaloye M. Geochemistry of nickel, cobalt and copper in alpine-type ultramafic rocks. Chem Geol 1976;17: 269–80.

[16] Miyashiro A. Volcanic rock series in island arcs and active continental margins. Am J Sci 1974;274:321–55.

[17] Jensen LS. A new cation plot for classifying sub- alkalic volcanic rocks. Ontario Dept. Mines Misc 1976;66:2.

[18] Peccerillo A, Taylor SR. Geochemistry of eocene calc-alkaline volcanic rocks from the Kastamanu area, northern Turkey. Contrib Mineral Petrol 1976;58:63–81.

[19] Maniar PD, Piccoli PM. Tectonic discrimination of granitoids. Geol Soc Am Bull 1989;101:635–43.

[20] Mullen ED. MnO/TiO2/P2O5; A minor element discriminant for basaltic rocks of oceanic environments and its implications for petrogenesis. Earth Planet Sci Lett 1983;62: 53−62.
[21] Shervais JW. Ti-V plots and the petrogenesis of modern and ophiolitic lavas. Earth Planet Sci Lett 1982;59:101−18.
[22] Pearce JA. In: Thorpe RS, editor. Trace element characteristics of lavas from destructive plate boundaries. Andesites: orogenic andesites and related rocks. New York: John Wiley & Sons; 1982. p. 525−54.
[23] Pearce JA, Norry MJ. Petrogenetic implications of Ti, Zr, Y and Nb variations in volcanic rocks. Contrib Mineral Petrol 1979;69:33−4.
[24] Taylor SR, McLennan SM. The continental crust: its composition and evolution. Blackwell; Oxford, United States 1985. p. 312.